Contribution from the Department of Chemistry,
West Virginia University, Morgantown, West Virginia 26506

Dilute Single-Crystal Electron Paramagnetic Resonance Study of $(\eta^5\text{-}C_5H_4CH_3)_2NbCl_2$. Observation of Cl Hyperfine Coupling with the Unpaired Electron

JEFFREY L. PETERSEN* and JAMES W. EGAN, JR.

Received January 26, 1983

A dilute single-crystal EPR study of $(\eta^5\text{-}C_5H_4CH_3)_2NbCl_2$ doped in the crystal lattice of $(\eta^5\text{-}C_5H_4CH_3)_2ZrCl_2$ was conducted to evaluate the spatial distribution of the unpaired electron from the orientation dependence of the ^{93}Nb hyperfine interaction. The g and hyperfine tensors not only are coincident for $(\eta^5\text{-}C_5H_4CH_3)_2NbCl_2$ but also exhibit the same molecular orientation as those in the corresponding d^1 vanadium system. The average magnetic parameters obtained for $(\eta^5\text{-}C_5H_4CH_3)_2NbCl_2$ are $g_x = 1.9754$, $g_y = 1.9396$, $g_z = 2.0018$, $T_x = (-)118.7$ G, $T_y = (-)178.4$ G, and $T_z = (-)59.0$ G. The large anisotropy observed for the ^{93}Nb hyperfine coupling interaction arises from an admixture of primarily $4d_{z^2}$ and some $4d_{x^2-y^2}$ character in the HOMO, where the z axis is defined as being normal to the plane that bisects the Cl–Nb–Cl bond angle. For certain orientations with the magnetic field parallel to the $NbCl_2$ plane of the doped crystal, additional splitting of the ^{93}Nb hyperfine lines due to Cl ligand hyperfine interaction was resolved. The origin of this interaction probably arises from a spin-polarization mechanism involving the Nb–Cl σ bonds.

Introduction

The electronic structure of bis(cyclopentadienyl)metal complexes, $(\eta^5\text{-}C_5H_5)_2ML_2$, has been investigated by a variety of spectroscopic and theoretical methods.[1] For appropriate paramagnetic derivatives electron paramagnetic resonance has provided quantitative information about the orbital character of the unpaired electron in the HOMO. For example, dilute single-crystal electron paramagnetic resonance studies of $(\eta^5\text{-}C_5H_5)_2VS_5$[2,3] and $(\eta^5\text{-}C_5H_4CH_3)_2VCl_2$[2,4] disclosed from an analysis of the orientation dependence of the ^{51}V hyperfine interaction that the unpaired electron resides in an a_1 molecular orbital of predominantly $3d_{z^2}$ and $3d_{x^2-y^2}$ metal character in these complexes. Although the relative contributions of these two metal orbitals to the observed anisotropy of the hyperfine interaction are dependent on the choice of coordinate system, the spatial orientation of the orbital obviously is not. In these particular d^1 organometallic systems, the unpaired electron is located in an orbital directed primarily along the normal to the plane that bisects the VL_2 bond angle.

During the course of the dilute single-crystal EPR measurements made for $(\eta^5\text{-}C_5H_4CH_3)_2VCl_2$, a large variation in the line width of the ^{51}V hyperfine lines was observed for spectra measured with the direction of the magnetic field parallel to the VCl_2 plane. Although no additional spectral features were resolved, the anisotropy of the spectral line width probably reflects a small unresolvable hyperfine interaction with the two Cl ligands. The possibility of this interaction is supported by the outcome of nonparameterized molecular orbital calculations on various $(\eta^5\text{-}C_5H_5)_2ML_2$ complexes,[5] which revealed that the molecular orbital of interest contains a reasonable contribution from the in-plane Cl p_π orbitals.

To investigate this interaction further, we have undertaken similar dilute single-crystal EPR studies of $(\eta^5\text{-}C_5H_4CH_3)_2NbCl_2$. Solution and frozen-glass EPR data[6-11] have been reported for a wide variety of $(\eta^5\text{-}C_5H_5)_2NbL_2$ complexes, which exhibit isotropic ^{93}Nb hyperfine coupling constants that range from 45 to 120 G. In some of these organoniobium complexes, such as $(\eta^5\text{-}C_5H_5)_2NbH_2$,[7] $(\eta^5\text{-}C_5H_5)_2Nb(CH_3)_2$,[7] and $(\eta^5\text{-}C_5H_5)_2Nb(C_5H_{10})$,[12] each of the 10 niobium hyperfine lines is split further by ^1H hyperfine coupling with the hydride ligand or α protons of the methyl ligand or metallacyclohexane ring. On the other hand, for $(\eta^5\text{-}C_5H_5)_2NbCl_2$, Cl ligand hyperfine interaction is not resolved in either the solution or frozen-glass spectra. This result is consistent with the small hyperfine splitting expected for unpaired spin density located in p orbitals of the Cl ligands.[13] In addition, since the principal axes of the magnetic tensors of the Nb and Cl hyperfine interactions are not likely to be coincident, one expects any spectral features due to the latter to be lost in a randomly oriented matrix. Despite these inherent problems, we felt that the larger radial extension of the Nb 4d orbitals compared to the V 3d orbitals might enhance the likelihood of resolving a Cl ligand hyperfine interaction for $(\eta^5\text{-}C_5H_4CH_3)_2NbCl_2$ in an oriented crystalline environment. The outcome of our EPR investigation is presented and further substantiates our previous extrapolation of the magnetic behavior for d^1 $(\eta^5\text{-}C_5H_5)_2VL_2$ complexes to the corresponding niobium systems.[4]

Experimental Section

Materials. All manipulations were performed under a dry nitrogen or Ar atmosphere with the aid of a double-manifold vacuum line. Solvents were purified by standard methods and freshly distilled prior to use. $ZrCl_4$ was purchased from Alfa Ventron whereas $NbCl_5$ and the methylcyclopentadienyl dimer were obtained from Aldrich.

Preparation of Compounds. Bis(methylcyclopentadienyl)zirconium dichloride and bis(methylcyclopentadienyl)niobium dichloride were prepared by procedures described in the literature for the corresponding bis(cyclopentadienyl)zirconium[14] and -niobium[15,16] analogues. To reduce contamination of the methylcyclopentadiene monomer by cyclopentadiene during the preparation of $NaC_5H_4CH_3$, the me-

(1) Lauher, J. W.; Hoffmann, R. *J. Am. Chem. Soc.* **1976**, *98*, 1729 and references cited therein.
(2) Petersen, J. L.; Dahl, L. F. *J. Am. Chem. Soc.* **1974**, *96*, 2248.
(3) Petersen, J. L.; Dahl, L. F. *J. Am. Chem. Soc.* **1975**, *97*, 6416.
(4) Petersen, J. L.; Dahl, L. F. *J. Am. Chem. Soc.* **1975**, *97*, 6422.
(5) Petersen, J. L.; Lichtenberger, D. L.; Fenske, R. F.; Dahl, L. F. *J. Am. Chem. Soc.* **1975**, *97*, 6433.
(6) (a) Stewart, C. P.; Porte, A. L. *J. Chem. Soc., Dalton Trans.* **1973**, *722*. (b) Stewart, C. P.; Porte, A. L. *Ibid.* **1972**, 1661.
(7) (a) Elson, I. H.; Kochi, J. K. *J. Am. Chem. Soc.* **1975**, *97*, 1262. (b) Elson, I. H.; Kochi, J. K.; Klabunde, U.; Manzer, L. E.; Parshall, G. W.; Tebbe, F. B. *Ibid.* **1974**, *96*, 7374.
(8) Hitchcock, P. B.; Lappert, M. F.; Milne, C. R. C. *J. Chem. Soc., Dalton Trans.* **1981**, 180.
(9) Manzer, L. E. *Inorg. Chem.* **1977**, *16*, 525.
(10) Kilmer, N. H.; Brubaker, C. H., Jr. *Inorg. Chem.* **1979**, *18*, 3283.
(11) Sanchez, C.; Vivien, D.; Livage, J.; Sala-Pala, J.; Viard, B.; Guerchais, J. E. *J. Chem. Soc., Dalton Trans.* **1981**, 64.
(12) Howard, K. E.; Petersen, J. L., unpublished results.
(13) Atkins, P. W.; Symons, M. C. R. "The Structure of Inorganic Radicals"; Elsevier: Amsterdam, 1967; pp 14–28.
(14) Eisch, J. J.; King, R. B. "Organometallic Synthesis"; Academic Press: New York, 1965; Vol. 1, p 75.
(15) Douglas, W. E.; Green, M. L. H. *J. Chem. Soc., Dalton Trans.* **1972**, 1796.
(16) Lucas, C. R. *Inorg. Synth.* **1976**, *16*, 107–109.

0020-1669/83/1322-3571$01.50/0

thylcyclopentadiene dimer was cracked according to a procedure described by Reynolds and Wilkinson.[17] The compounds were purified either by recrystallization from $CHCl_3$ or by high-vacuum sublimation.

Characterization of Compounds. $(\eta^5\text{-}C_5H_4CH_3)_2ZrCl_2$ was characterized by ^1H and ^{13}C NMR measurements recorded on a Varian CFT-20 NMR spectrometer operating in the FT mode. The ^1H and ^{13}C NMR spectra are analogous to those reported by Stucky and co-workers[18] for alkyl-substituted zirconocene dichlorides. ^1H NMR spectrum ($CDCl_3$): δ 2.21 (CH_3, singlet), 6.13 (triplet, $J_{H-H} \sim 3$ Hz), 6.30 (triplet, $J_{H-H} \sim 3$ Hz). ^{13}C NMR spectrum ($CDCl_3$): δ 15.33 (methyl carbon), 112.39, 117.53, and 130.22 (ring carbons).

The solution EPR spectrum of $(\eta^5\text{-}C_5H_4CH_3)_2NbCl_2$, which was recorded on a Varian E-3 spectrometer, exhibits the characteristic 10-line spectrum due to the hyperfine interaction of the unpaired electron with the ^{93}Nb nucleus (100%, $I = {}^9/_2$). The isotropic EPR parameters calculated from a modified form of the Breit–Rabi equation[19] are $g_{iso} = 1.9842$ and $A_{iso} = (-)113.7$ G and are comparable to the corresponding values reported for $(\eta^5\text{-}C_5H_5)_2NbCl_2$.[6,7]

Structural Analysis of Host Crystal Lattice. To undertake a dilute single-crystal EPR study, an appropriate diamagnetic host material with a molecular structure similar to that of the paramagnetic compound must be used. For this particular study $(\eta^5\text{-}C_5H_4CH_3)_2ZrCl_2$ was chosen since large diamond-shaped crystals can be readily obtained by the cooling of a saturated chloroform solution. To determine the spatial arrangement of the $(\eta^5\text{-}C_5H_4CH_3)_2ZrCl_2$ in the crystal lattice, a single-crystal X-ray diffraction analysis of $(\eta^5\text{-}C_5H_4CH_3)_2ZrCl_2$ was undertaken. Preliminary oscillation and Weissenberg photographs of a crystal of appropriate dimensions were measured with Ni-filtered Cu Kα radiation and showed the Laue symmetry to be orthorhombic D_{2h}-$2/m\,2/m\,2/m$. Systematic absences for $\{0kl\}$ of $k + l = 2n + 1$ and for $\{hk0\}$ of $h = 2n + 1$ are compatible with two possible space groups, *Pnma* (D_{2h}^{16} No. 62) and *Pna*2_1 (C_{2v}^9 No. 33). The lattice parameters for $(\eta^5\text{-}C_5H_4CH_3)_2ZrCl_2$ were determined and found to be analogous to those reported for $(\eta^5\text{-}C_5H_4CH_3)_2TiCl_2$,[4,20] indicating that their crystal lattices are isomorphous. A subsequent structural analysis, the details of which are included as supplementary material with the other structural data, substantiated this observation. The fact that our host lattice conforms to the same crystal system as $(\eta^5\text{-}C_5H_4CH_3)_2TiCl_2$ greatly simplifies the acquisition and interpretation of the EPR data.

Single-Crystal EPR Measurements. Suitable single crystals of $(\eta^5\text{-}C_5H_4CH_3)_2ZrCl_2$ doped with ca. 1% of $(\eta^5\text{-}C_5H_4CH_3)_2NbCl_2$ were grown from a chloroform solution by slow evaporation of solvent under a prepurified stream of dry nitrogen. The crystals have well-defined external morphology and were found by X-ray diffraction photographs to possess the same Laue symmetry and cell dimensions of the host material. The crystal used for the EPR measurements was placed in a locally made crystal orientation device constructed to provide two orthogonal rotational degrees of freedom. This capability is accomplished by grinding a circular groove across one end of a 6-mm-diameter quartz tube to accommodate a quartz cylinder of 6-mm length. The quartz cylinder is mounted perpendicular to the tube and is supported by a spring-loaded loop of silk thread. Turning of a threaded metal arm at the other end of the quartz tube permits one to rotate simultaneously the quartz cylinder in which the doped crystal is placed. The other degree of freedom is obtained by rotation about the spindle axis of the quartz tube. The amount of rotation is measured from a 12-in. full-circle protractor marked in 0.5° divisions that is centered at the base of the goniometer. Since these two degrees of freedom permit any orientation of the crystal with respect to the magnetic field direction, the crystal could be oriented along the *a*, *b*, or *c* crystallographic axis such that each was within 0.5° of being parallel to the principal spindle axis of the goniometer. The sample was placed in a Varian rectangular microwave cavity between the pole faces of the 4-in. magnet of a Varian E-3 spectrometer. The orientation of the crystal with respect to the magnetic field direction was changed by a clockwise rotation about the spindle axis of the crystal holder. A 2000-G scan of 1-h duration was obtained at room temperature for every 10° rotation about each of the crystallographic axes. One 10-line spectrum was observed for orientations where the magnetic field direction is perpendicular to either the *a* or *c* axis, while for orientations about the *b* axis two overlapping 10-line spectra were observed. Figure 1 depicts two representative EPR spectra obtained for $(\eta^5\text{-}C_5H_4CH_3)_2NbCl_2$ diluted in $(\eta^5\text{-}C_5H_4CH_3)_2ZrCl_2$ taken with the *b* axis parallel and perpendicular to the magnetic field, respectively. As indicated in Figure 1B, it is evident that the line widths of the hyperfine lines are orientation dependent. The observed variation from 6 to 20 G reflects the presence of hyperfine components due to an interaction with the ^{35}Cl (75.5% abundance, $I = {}^3/_2$) and ^{37}Cl (24.5% abundance, $I = {}^3/_2$) nuclei. In fact, for some of the spectra measured about the *b* axis additional structure superimposed upon the niobium hyperfine lines was partially resolved. Figure 2 represents one of the niobium lines recorded at $\theta = 150°$ for site B (i.e., along the T_x direction that bisects the Cl–Nb–Cl bond angle). At this

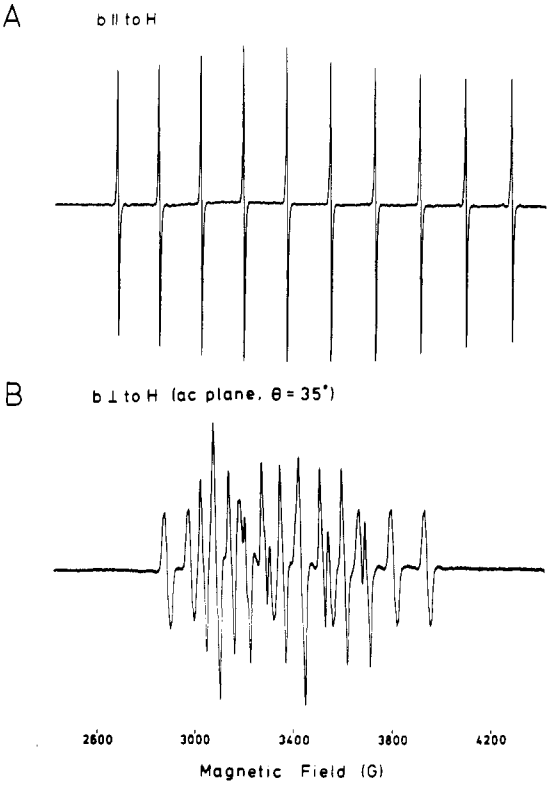

Figure 1. Single-crystal EPR spectra of $(\eta^5\text{-}C_5H_4CH_3)_2NbCl_2$ doped into the crystal lattice of $(\eta^5\text{-}C_5H_4CH_3)_2ZrCl_2$ with (A) the crystallographic *b* axis parallel and (B) the *b* axis perpendicular ($\theta = 35°$) to the direction of the magnetic field.

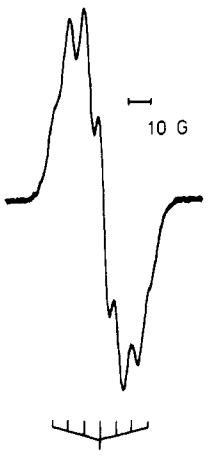

Figure 2. One of the ten ^{93}Nb hyperfine lines from the single-crystal EPR spectrum measured with the magnetic field directed along T_x. Since the two Cl atoms are magnetically equivalent here, each niobium line is split into seven additional lines due to Cl ligand hyperfine coupling.

(17) Reynolds, L. T.; Wilkinson, G. *J. Inorg. Nucl. Chem.* **1959**, *9*, 86.
(18) Davis, J. H.; Sun, H.; Redfield, D.; Stucky, G. *J. Magn. Reson.* **1980**, *37*, 441.
(19) Weil, J. A. *J. Magn. Reson.* **1971**, *4*, 394.
(20) The refined lattice parameters for $(\eta^5\text{-}C_5H_4CH_3)_2ZrCl_2$ are $a = 12.033$ (3) Å, $b = 15.539$ (4) Å, $c = 6.904$ (1) Å, and $V = 1291.0$ (6) Å^3 with four molecules per unit cell and $\rho_{calcd} = 1.648$ g/cm^3.

Table I. Final Analysis of Single-Crystal EPR Data Obtained for the Two Magnetically Nonequivalent $(\eta^5\text{-}C_5H_4CH_3)_2NbCl_2$ Molecules Doped into the Diamagnetic $(\eta^5\text{-}C_5H_4CH_3)_2ZrCl_2$ Host

	site A		site B	
	g^2	10^5K^2, MHz^2	g^2	10^5K^2, MHz^2
P_a	3.984 29	1.768 58	3.984 29	1.768 58
Q_a	3.762 68	8.842 73	3.762 68	8.842 73
R_a	0.001 26	0.054 82	0.001 26	0.054 82
P_b	3.925 54	3.441 82	3.926 45	3.428 30
Q_b	3.983 45	1.867 81	3.982 64	1.856 46
R_b	0.046 10	−1.346 58	−0.044 06	1.331 61
P_c	3.761 37	8.809 20	3.761 37	8.809 20
Q_c	3.928 59	3.434 23	3.928 59	3.434 23
R_c	0.002 49	−0.005 46	0.002 49	−0.005 46

principal values[a,b]	direction cosines[c]		
	Site A		
$g_x = 1.9752$	0.872	−0.014	0.489
$g_y = 1.9396$	0.011	1.000	0.009
$g_z = 2.0019$	−0.489	−0.003	0.872
$T_x = (-)118.9$ G	0.867	−0.004	0.498
$T_y = (-)178.4$ G	0.007	1.000	−0.005
$T_z = (-)59.0$ G	−0.498	0.008	0.867
	Site B		
$g_x = 1.9756$	−0.875	−0.018	0.485
$g_y = 1.9396$	−0.020	1.000	0.000
$g_z = 2.0017$	−0.484	−0.009	−0.875
$T_x = (-)118.5$ G	−0.869	0.000	0.495
$T_y = (-)178.4$ G	0.004	1.000	0.006
$T_z = (-)59.0$ G	−0.495	0.007	−0.869

[a] Principal values of the ^{93}Nb hyperfine tensor were converted from units of MHz to gauss (G) by using the relationship T_i (G) = 2.00232T_i (MHz)/2.80247g_i. [b] The esd's for the principal components of **g** and **T** are ±0.0005 and ±0.5 G, respectively. [c] The eigenvectors are unique to within a sign change for each column.

orientation, the two chlorine ligands are magnetically equivalent as evidenced by the $(2)(2)(^3/_2) + 1$ or seven hyperfine lines that are separated by ca. 7.5 G. However, as the crystal is rotated away from $\theta = 150°$, the Cl atoms become nonequivalent with an accompanying loss of resolution within a 30° rotation.

No evidence of weak resonance lines due to "forbidden" transitions ($\Delta m_s = \pm 1$, $\Delta m_I = \pm 1$) was observed. The resonance magnetic field at each of the hyperfine lines was determined from a manual scan of the magnetic field with the magnetic field dial and recording the dial setting at the center of each line position. The microwave frequency was monitored with a Hewlett-Packard X532B frequency meter positioned within the waveguide. The magnetic field strength of the spectrometer was calibrated by using a polycrystalline DPPH sample ($g = 2.0036$) or a chloroform solution of $(\eta^5\text{-}C_5H_4CH_3)_2VCl_2$ ($g_{iso} = 1.9864$ and $A_{iso} = (-)74.5$ G) in conjunction with the frequency meter.

Analysis of the EPR Data. The dilute single-crystal EPR spectra measured for $(\eta^5\text{-}C_5H_4CH_3)_2NbCl_2$ were analyzed by using the computational procedure as described previously in detail for $(\eta^5\text{-}C_5H_5)_2VS_5$.[3] The components of the $\mathbf{g}^2$ and $\mathbf{K}^2 = \mathbf{g}^2\mathbf{T}^2$ matrices (Table I) for the two nonequivalent magnetic sites of $(\eta^5\text{-}C_5H_4CH_3)_2NbCl_2$ in the host crystal lattice were determined from a least-squares fit[21] of the corrected magnetic data[22] to the three-parameter equation

$$Y_i = P\cos^2\theta_i + Q\sin^2\theta_i - 2R\sin\theta_i\cos\theta_i$$

where $Y_i = g^2$ or K^2 and θ_i = angle of rotation. The results of this least-squares analysis are depicted in Figure 3, which illustrates the angular dependence of the g and the ^{93}Nb hyperfine coupling parameters.

After the principal values and the orientation of the electron Zeeman and the hyperfine coupling tensors were determined, the correctness of the analysis was checked by the calculation of the magnetic fields

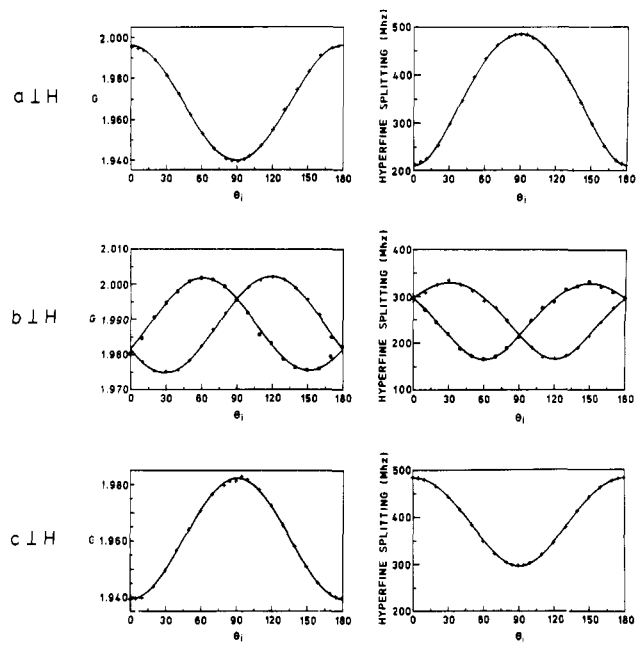

Figure 3. Plots of experimental g and hyperfine splitting values (in MHz) as a function of the angle of rotation, θ_i, for the three orthogonal sets of EPR data. The solid curves represent the best fit of the experimental data (crosses, site A; solid circles, site B) to a three-parameter equation, $P\cos^2\theta_i + Q\sin^2\theta_i - 2R\sin\theta_i\cos\theta_i$.

for the ^{93}Nb hyperfine lines of each spectrum. A comparison of the experimental line positions with those calculated by a second-order perturbation computation indicated agreement for most resonance lines for $(\eta^5\text{-}C_5H_4CH_3)_2NbCl_2$ to within 2 G.

Discussion of Results

Molecular Structure of $(\eta^5\text{-}C_5H_4CH_3)_2ZrCl_2$. The X-ray structure determination of $(\eta^5\text{-}C_5H_4CH_3)_2ZrCl_2$ did not reveal any unusual structural features. The pseudo-tetrahedral coordination environment about the central Zr atom is characterized by the following structural parameters: Cp(c)–Zr = 2.206 (5) Å, Zr–Cl = 2.443 (1) Å (average), Cp(c)–Zr–Cp′(c) = 128.9 (2)°, and Cl–Zr–Cl = 95.10 (5)°, where Cp(c) refers to the ring centroid and the prime indicates the appropriate symmetry-related position. These parameters are comparable to those reported by Green et al.[23] for $(\eta^5\text{-}C_5H_5)_2ZrCl_2$ and therefore deserve no further comment.

Discussion and Interpretation of EPR Data. From the structural analysis of $(\eta^5\text{-}C_5H_4CH_3)_2ZrCl_2$, the orientation of the four molecules in the unit cell is analogous to that for $(\eta^5\text{-}C_5H_4CH_3)_2TiCl_2$. Each molecule lies on a crystallographic mirror plane, which parallels the *ac* plane and contains the MCl_2 molecular fragment. Consequently, upon doping of the host lattice with $(\eta^5\text{-}C_5H_4CH_3)_2NbCl_2$, the paramagnetic species conforms rigorously to C_s-*m* site symmetry. Under these circumstances, the number of magnetically nonequivalent sites is reduced from 2 for spectra measured with $\vec{H}$ perpendicular to the *b* axis to 1 for spectra measured with $\vec{H}$ perpendicular to the *a* or *c* axis. As a result of this crystallographically imposed constraint, one principal axis of each magnetic tensor must be normal to the mirror plane containing the niobium and two chlorine atoms. The remaining two principal axes are constrained to lie within the $NbCl_2$ plane.

A comparison of the EPR data plotted in Figure 3 for $(\eta^5\text{-}C_5H_4CH_3)_2NbCl_2$ with those obtained for $(\eta^5\text{-}C_5H_4CH_3)_2VCl_2$ reveals that the metal hyperfine interactions in both systems display the same orientation dependence. An examination of the Eulerian angles (Φ, Θ, and Ψ)[24] given in

(21) Farach, H. A.; Poole, C. P., Jr. *Adv. Magn. Reson.* **1971**, *5*, 229.
(22) Weil, J. A.; Goodman, G. L.; Hecht, H. G. "Paramagnetic Resonance"; Low, W., Ed.; Academic Press: New York, 1963; p 880.
(23) Green, J. C.; Green, M. L. H.; Prout, C. K. *J. Chem. Soc., Chem. Commun.* **1972**, 421 and references cited therein.

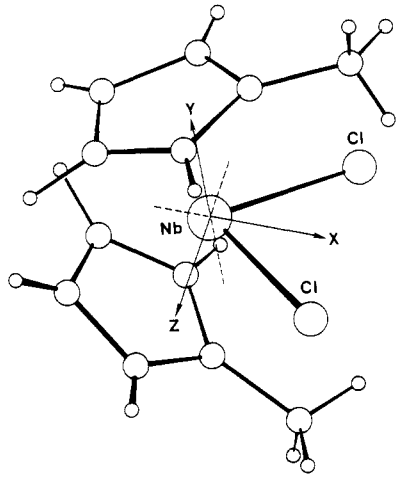

Figure 4. Orientation of the principal axes for the magnetic tensors with respect to the molecular structure of $(\eta^5\text{-}C_5H_4CH_3)_2NbCl_2$.

Table II. Best-Fit Values for Magnetic Parameters Obtained from Single-Crystal EPR Study of $(\eta^5\text{-}C_5H_4CH_3)_2NbCl_2$

Principal Values	
$g_x = 1.9754$	$T_x = (-)118.7$ G
$g_y = 1.9396$	$T_y = (-)178.4$ G
$g_z = 2.0018$	$T_z = (-)59.0$ G

Other EPR Parameters (for $a = -0.967$ and $b = 0.255$)

$K = 107.7 \times 10^{-4}$ cm^{-1}	$\chi = -3.72$
$P = 107.0 \times 10^{-4}$ cm^{-1}	$\lambda \sim 110$ cm^{-1}
$\langle r^{-3} \rangle = 2.46$ au	

$$a^2/b^2 = -0.967^2/0.255^2 = 14.4$$

Table I not only indicates that the principal axes of the **g** and **T** tensors are coincident for $(\eta^5\text{-}C_5H_4CH_3)_2NbCl_2$ but also substantiates that their molecular orientations are the same for $(\eta^5\text{-}C_5H_4CH_3)_2VCl_2$ and $(\eta^5\text{-}C_5H_4CH_3)_2NbCl_2$, as one would expect. The actual orientation of the principal directions for the magnetic tensors with respect to the molecular geometry of $(\eta^5\text{-}C_5H_4CH_3)_2NbCl_2$ is illustrated in Figure 4. In terms of our coordinate system, the x component bisects the Cl–Nb–Cl bond angle, the y component is normal to the $NbCl_2$ plane, and the z component is normal to the xy plane, which bisects the Cl–Nb–Cl bond angle.

The average principal values for the **g** and **T** tensors for the two nonequivalent magnetic sites of $(\eta^5\text{-}C_5H_4CH_3)_2NbCl_2$ are provided in Table II. On the basis of the same ligand field model previously used[4] to analyze the single-crystal EPR data for $(\eta^5\text{-}C_5H_4CH_3)_2VCl_2$, the metal orbital character of the unpaired electron and the other EPR parameters, including λ, χ, P, K, and $\langle r^{-3} \rangle$, can be calculated from the principal values obtained for the **g** and **T** tensors. For an electronic ground state described to a first approximation as $|\Phi_0\rangle = a|4d_{z^2}\rangle + b|4d_{x^2-y^2}\rangle$, the optimal values of the mixing coefficients, a and b, can be adjusted to minimize the difference between the calculated and observed values for the principal components of the magnetic tensors. The unique set of values for a and b indicates that the unpaired electron resides in a metal-based molecular orbital composed primarily of $4d_{z^2}$ with a small contribution from the $4d_{x^2-y^2}$. Although the relative contributions of these two 4d orbitals to the HOMO are drastically different, as illustrated by the ratio of their percent character, $a^2/b^2 = 14.4$, one must be reminded that the calculated values for a and b are dependent upon the choice of the axis-labeling scheme and therefore are not rotationally invariant. Since the orientation of the principal axes of the magnetic tensors are known with respect to the molecular

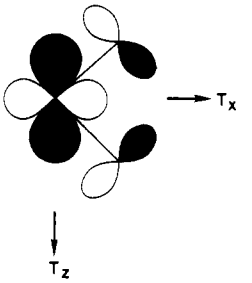

Figure 5. Orbital representation depicting π-antibonding interaction between hybridized metal and in-plane Cl p orbitals for HOMO in $(\eta^5\text{-}C_5H_4CH_3)_2NbCl_2$.

geometry in this case from the dilute single-crystal EPR data, the necessary transformation to determine the effect of a simple permutation of axis labels upon the values of a and b is trivial and has been discussed elsewhere.[3,4] However, for molecular systems where the orientation of the magnetic tensors is not known unambiguously, an arbitrary assignment can lead to an incorrect interpretation. This situation frequently arises during the analysis of frozen-glass or dilute-powder EPR spectra of paramagnetic systems with nonaxial symmetry. Illustrating this problem is one of the earliest papers[6a] devoted to EPR studies of $(\eta^5\text{-}C_5H_5)_2ML_2$ complexes, where M = V or Nb. Although their computer simulation of the frozen-glass EPR spectra provided reasonable values of the principal components for the **g** and **T** tensors, their assignment of the principal directions for these tensors appears to have been an arbitrary one. In this case, the principal axis with the largest g value and smallest T value (i.e., z component in terms of our coordinate system) was presumed to coincide with the C_2-2 symmetry axis that bisects the L–M–L bond angle in the molecule. More recently, a paper describing the frozen-glass spectra for $[(\eta^5\text{-}C_5H_5)_2Nb(S_2P(OR)_2)]^+$ complexes (R = Et, *i*-Pr) involves a similar problem.[11] Although the anisotropy of the ^{93}Nb hyperfine interaction in these complexes containing a planar NbS_2P heteroatom ring might be expected to vary from that observed for $(\eta^5\text{-}C_5H_4CH_3)_2NbCl_2$, it unlikely the spatial orientation of the unpaired electron (as dictated by the metal orbital character of the HOMO) would change as dramatically as suggested here. Their conclusions are based on an arbitrary assumption that the smallest g value and largest T value (i.e., y component in terms of our coordinate system) correspond to the principal axis that bisects the S–Nb–S angle. Consequently, the conclusions drawn about the spatial distribution of the unpaired electron in both cases are inconsistent with the general picture that has developed during the past decade for the electronic structure of $(\eta^5\text{-}C_5H_5)_2ML_2$ complexes and related derivatives.[1]

Origin of Cl Hyperfine Interaction. For certain orientations of the doped crystal with respect to the magnetic field direction, additional splitting of the ^{93}Nb hyperfine lines due to a Cl hyperfine interaction was resolved. The origin of this interaction can be better understood after a brief review of the molecular orbital representation that has developed for $(\eta^5\text{-}C_5H_5)_2ML_2$ complexes. From crystallographic data[4,23,25-28] gathered for a considerable number of $(\eta^5\text{-}C_5H_5)_2ML_2$ complexes, a structural correlation was recognized between the

(24) Goldstein, H. "Classical Mechanics"; Wiley: New York, 1965; p 107.

(25) (a) Muller, E. G.; Petersen, J. L.; Dahl, L. F. *J. Organomet. Chem.* **1976**, *111*, 91. (b) Muller, E. G.; Watkins, S. F.; Dahl, L. F. *Ibid.* **1976**, *111*, 73.

(26) Prout, C. K.; Camerson, T. S.; Forder, R. A.; Critchley, S. R.; Denton, B.; Rees, G. V. *Acta Crystallogr., Sect. B* **1974**, *B30*, 2290.

(27) Clearfield, A.; Warner, D. K.; Saldarriaga-Molina, C. H.; Ropal, R.; Bernal, I. *Can. J. Chem.* **1975**, *53*, 1622 and references cited therein.

(28) Atwood, J. L.; Rogers, R. D.; Hunter, W. E.; Floriani, C.; Fachinetti, G.; Chiesa-Villa, A. *Inorg. Chem.* **1980**, *19*, 3812 and references cited therein.

electron configuration of the metal and the length of the M–L bond. As the number of nonbonding electrons on the metal increases from a d^0 (Ti, Zr) to d^1 (V, Nb) to d^2 (Mo) system, a lengthening of the M–L bond is observed for metals from the same period. This trend, which is contrary to what is expected on the sole basis of covalent radii considerations, strongly suggests that an antibonding interaction between the metal and ligand orbitals develops as the HOMO becomes populated. This remark has been further supported by nonparameterized MO calculations that indicate a small but significant antibonding contribution from the in-plane Cl p_π orbitals to the HOMO for $(\eta^5\text{-}C_5H_5)_2MCl_2$ complexes, where M = Ti, V, or Mo.[5] An orbital diagram that incorporates this contribution is shown in Figure 5. From this representation the origin of the Cl ligand hyperfine interaction cannot arise from a direct π overlap of the metal and Cl p_π orbitals since a positive overlap between these orbitals does not exist. If the latter situation were present, a much larger coupling interaction would have been expected than what was observed. With this in mind, a more appropriate rationalization for the Cl hyperfine interaction is that it probably occurs via a spin-polarization mechanism involving the Nb–Cl σ bonds. Alternative mechanisms involving contributions from appropriate excited electronic configurations are less attractive due to unfavorable energetics.

When the magnetic field direction parallels the T_x axis of the ^{93}Nb hyperfine tensor, the two Cl ligands are equivalent and seven equally spaced lines are observed. However, as the crystal is rotated in either a clockwise or counterclockwise manner, the magnetic field direction no longer makes the same angle with the principal axes of the Cl hyperfine tensors (which are probably oriented along and perpendicular to the Nb–Cl bonds). Under these circumstances, as the magnitudes of the individual hyperfine interaction from the two Cl ligands become more widely different, the resolvability of their corresponding spectral lines diminishes.

Concluding Remarks. The outcome of this EPR analysis has substantiated our earlier premise that the principal axes of the **g** and hyperfine tensors in $(\eta^5\text{-}C_5H_4CH_3)_2VCl_2$ and $(\eta^5\text{-}C_5H_4CH_3)_2NbCl_2$ are identical.[4] For our choice of coordinate system, the z direction (which corresponds to the largest g value and smallest absolute T value) is defined as being directed perpendicular to the plane that bisects the Cl–M–Cl bond angle in these systems. This assignment was made originally to simplify the comparison of the metal orbital character as determined by single-crystal EPR methods with qualitative bonding models proposed by Ballhausen and Dahl[29] and Alcock.[30] In the latter case, the HOMO containing the unpaired electron for these d^1 systems was presumed to be a pure nd_{z^2} orbital, in terms of our coordinate system. From these EPR studies an additional, small but significant contribution from the corresponding $nd_{x^2-y^2}$ orbital is present. The resultant admixture of these two metal d orbitals places the unpaired electron in a metal-based MO orbital that lies within the ML_2 plane. With this in mind, one would expect that the anisotropy of the hyperfine interaction in these paramagnetic organometallic complexes be sensitive to stereochemical alterations since the relative contributions of these two AO's (as determined by a and b) are dependent upon the nature of the metal–ligand interaction and the resultant L–M–L bond angle.[31] Further studies are in progress to examine the extent of this correlation.

Acknowledgment. Partial support of this work by the National Science Foundation (Grant No. IPS-8011453) is acknowledged. Computer time for the X-ray diffraction and EPR data analyses was provided by the West Virginia Network for Educational Telecomputing.

Registry No. $(\eta^5\text{-}C_5H_4CH_3)_2ZrCl_2$, 12109-71-6; $(\eta^5\text{-}C_5H_4CH_3)_2NbCl_2$, 61374-51-4.

Supplementary Material Available: Brief description of the X-ray structure analysis for $(\eta^5\text{-}C_5H_4CH_3)_2ZrCl_2$ and tables of positional and thermal parameters, bond distances and angles, and observed and calculated structure factors (13 pages). Ordering information is given on any current masthead page.

(29) Ballhausen, C. J.; Dahl, J. P. *Acta Chem. Scand.* **1961**, *15*, 1333.
(30) Alcock, N. W. *J. Chem. Soc. A* **1967**, 2001.
(31) Petersen, J. L.; Griffith, L. *Inorg. Chem.* **1980**, *19*, 1852.